Energy Research Journal

Original Research Paper

Modeling and Performance Analysis of a Petroleum-Pipeline-Pressure-Boosting Station Powered by Two-Shaft GT Engine

Yousef S. H. Najjar, Mohammad Z. M. Yousef and Aad M. A. Al-Mahgari

Department of Mechanical Engineering, Jordan University of Science and Technology, Irbid, Jordan

Article history
Received: 01-05-2021
Revised: 06-05-2021
Accepted: 18-05-2021

Corresponding Author:
Yousef S. H. Najjar
Department of Mechanical Engineering, Jordan University of Science and Technology, Irbid, Jordan
Email: y_najjar@hotmail.com

Abstract: This study offers modeling and performance analysis of a pressure-boosting station for petroleum pipelines using a sustainable two-shaft GT engine to drive a three-stage centrifugal pump. The modeling is divided into three steps; matching the GT engine components at the maximum efficiency line, matching the pump performance with the requirements of the pipeline system to generate the pump load curve, then matching the pump load curve to the GT engine power-speed curve at the maximum efficiency to study the plant's overall performance. At design point, the GT engine efficiency was 37.5% while the station net pumping-power output was ~ 2 MW with an overall efficiency of ~ 30% and Specific Fuel Consumption (SFC) of ~ 0.217 kg/kWh. Also, the effect of varying the GT engine compression ratio (r_c) on the plant's performance parameters, i.e., SFC, efficiency and power output were thoroughly examined, revealing that the compressor turbine range was the most limited and that the part-load efficiency of GT engine at 50% power-output loading was 32.2%. Finally, sensitivity analysis was performed to find that for each 10% drop in r_c, the station overall efficiency drops by only 6.5%.

Keywords: Petroleum Pipelines, Oil and Gas Transport, Two-Shaft Gas Turbine Modeling, Heat Exchange Cycle, Free-Power Turbine and Pressure-Boosting Station

Introduction

With the continuous rise of global population and the booming in urban and industrial development, the demand for energy is growing faster than ever. According to International Energy Agency (IEA), Oil and natural Gas (O&G) will continue to dominate the energy market at least for the first half of the 21st century despite the rising contribution of renewables, driven by stern environmental concerns (Hart, 2014). Moreover, the limitations and low market competitiveness of renewables make other approaches necessary. This include waste heat utilization through adopting various configurations (Akyurt *et al*., 1995; Barigozzi *et al*., 2015) to improve the efficiency and reduce CO_2 emissions.

On the other hand, one of the major aspects of O&G industry, beside production, is transporting the product over large distances using safe, less polluting and economically effective methods. Previous studies concluded that transporting O&G by tankers consumes large amounts of energy and contributes to increasing greenhouse gas levels. Therefore, using pipelines for O&G transporting has been proven to be safer, faster, cheaper and more sustainable (Wang *et al*., 2019; Guo *et al*., 2016). Pipelines are used to carry oil from production wells to refineries or from refineries to consumers over thousands-of-kilometers-long distances. However, such large distances lead to a significant pressure drop in the pipeline system, which increases with flow velocity but decreases with pipe diameter and temperature. This pressure loss is mainly caused by high oil viscosity, drag & shear forces with pipe walls and blocking formed by wax crystallization, especially when transporting heavy crude oil (Wang *et al*., 2019; Koch *et al*., 2015).

Losses which are created by high oil viscosity, drag and friction between oil and pipeline walls are treated by adding drag reducing additives (surfactants, fibers and polymers) (Gudala *et al*., 2019). Other solutions include dilution and emulsification (oil-in-water and water-in-oil emulsion) as well as heated pipelines to reduce viscosity (Martínez-Palou *et al*., 2011; Bensakhria *et al*., 2004). For example, the Core Annular Flow system (CAF) greatly reduces flow viscosity, because adding a thin film of water near the internal pipe wall lubricates the internal oil core. However, this heat adds extra costs and thermal losses and may induce changes in the crude oil rheological properties which creates instability in the flow (Bensakhria *et al*., 2004). In addition to the pressure drop

Science Publications

© 2021 Yousef S. H. Najjar, Mohammad Z. M. Yousef and Aad M. A. Al-Mahgari. This open access article is distributed under a Creative Commons Attribution (CC-BY) 4.0 license.

caused by frictional losses, there is also the variation in elevation due to the geographical nature of the pipeline route. Therefore, to maintain the oil flow and prevent critical pressure-drop values, many pressure-boosting stations should be installed along the pipeline route to raise the pumping pressure (Wang *et al*., 2019). The pumping power at each station can be supplied by a turbine, preferably a gas turbine, to drive a pump or compressor.

The advantage of using a Gas Turbine (GT) as a compressor or pump mover has been recognized very early due to its adjustable speed, low maintenance & installation costs and the ability to use the transmitted product as fuel. Moreover, GT output capacity grows in cold weather, thus, compensating for the increase in the demand for heating power in winter (Sawyer, 1976). The GTs are very popular in electricity-generating power plants, cogeneration, turbojet engines, naval propulsion, O&G transmission lines and large capacity district heating/cooling facilities (Chapman *et al*., 2016; Aklilu and Gilani, 2010; Al-Hamdan and Ebaid, 2006). Nevertheless, the poor GT part-load performance has led to utilizing different GT arrangements for further improvements, like controlled guide vanes, variable geometry turbines and multi-shaft designs (Poullikkas, 2005; Najjar and Abubaker, 2015; Mallinson and Lewis, 1948; Bălănescu and Homutescu, 2019; Najjar *et al*., 1993).

This study provides detailed modeling and analysis for a pressure-boosting station of a petroleum pipeline system using a two-shaft GT engine which operates on a heat-exchange cycle to drive a three-stage centrifugal pump. The variation in the GT parameters, such as compressor speed, compressor pressure ratio, turbine inlet temperature, specific fuel consumption, power output and efficiency, over a wide loading range was thoroughly investigated. This study can be summarized into three main steps: (1) Matching the GT engine components to optimize its performance and draw the "Power-Speed Curve", (2) matching the pipeline-system-requirements with the pump performance-map to generate the "Pump-Load Curve", (3) matching the GT "Power-Speed Curve" with the "Pump-Load Curve" to study the station overall performance. Also, a sensitivity analysis was carried out and the required calculations were implemented using Octave program.

Plant Description

To simplify the analysis and understand the working principles of the proposed pressure-boosting station, the system was divided into three parts: The two-shaft GT engine, the centrifugal pump and the pipeline. Figure 1 shows the components of the chosen GT engine connected to the centrifugal pump through a Gear Box (G.B). The two-shaft GT engine consists of two parts; the first is a Gas Engine (G.E), which comprises a compressor axially connected to a Compressor Turbine (CT) to provide the work required to drive the compressor. The second is a Power-Turbine (PT) connected to the load (G.B) on a separate shaft. This two-shaft design allows PT to rotate freely independent from the CT, thus enhancing the GT engine part-load efficiency compared with that of a single-shaft arrangement, especially for applications where the load requires a variable speed driver.

Air is sucked at point 1, compressed to high pressure (point 2) and preheated in the Heat exchanger (H.X) before it enters the Combustion Chamber (C.C) (point 6). It is then mixed with fuel under very high pressure. At this point, the combustion is initiated, producing very hot exhaust gases (point 3) that expand through the CT, providing the needed mechanical work to drive the compressor.

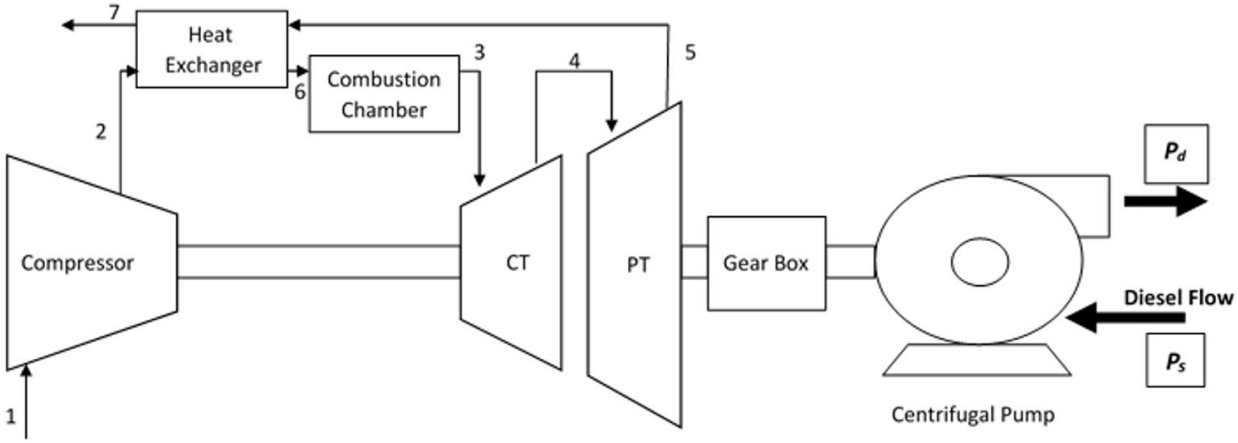

Fig. 1: A schematic diagram of the proposed pressure-boosting station driven by GT engine

The exhaust gases coming out of CT (point 4) expand further in the PT to provide the mechanical work that drives the second shaft, which is connected to the load (G.B). Since pumps usually operate at lower rotational speeds than turbines, the G.B functions as speed reducer to make PT speed compatible with the pump speed. The pump converts the received mechanical input power into a hydraulic pumping power used to raise the pressure of the oil inside the pipeline to compensate for the pressure drop and maintains the flow.

Methodology and Mathematical Modeling

In this section, the mathematical modeling of the petroleum pressure-boosting station is presented. The mathematical model includes the thermodynamic and fluid mechanics analyses of the two-shaft GT engine, centrifugal pump and the pipeline system are discussed. In addition, the matching process of all components of the proposed pressure-boosting station is described in this section. The brief flowchart shown in Fig. 2 shows the steps sequence which was used during work.

GT Engine Thermodynamic Analysis

The GT engine is thermodynamically modelled using equations given in (Cohen *et al*., 1987) and performance maps retrieved from (Turbocompressor, 2016) for the compressor and from (Smooth Turbine Maps, 2018) for the CT and PT. Scaling techniques provided by (Chapman *et al*., 2016; Gilani *et al*., 2008) were used to match the CT and PT performance maps with the GT design-point.

a) Compressor

The rise in air temperature and the work required during the compression process are given by Eq. (1) and Eq. (2), respectively.

$$\Delta T_{12} = \frac{T_1}{\eta_c} \times \left(r_c^{\frac{k_a - 1}{k_a}} - 1 \right) \tag{1}$$

$$W_c = m \times C_{p,a} \times \Delta T_{12} \tag{2}$$

b) Heat Exchanger (H.X)

The rise in temperature of the cold fluid stream, decrease in temperature of the hot fluid stream and the pressure drop across the H.X are given by Eq. (3), Eq. (4) and Eq. (5), respectively.

$$T_6 - T_2 = \epsilon \times (T_5 - T_2) \tag{3}$$

$$T_5 - T_7 = \epsilon \times \frac{C_{p,a}}{C_{p,g}} \times (T_5 - T_2) \tag{4}$$

$$\begin{aligned} \Delta P_{ha} &= P_2 \times \frac{\Delta P_{ha}}{P_2} (air\ side) \\ \Delta P_{hg} &= 0.01 Bar\ (gas\ side) \end{aligned} \tag{5}$$

c) Combustion Chamber (C.C)

By applying mass and energy balance across the C.C, the fuel-air-ratio (*f*) is calculated using Eq. (6) and the pressure drop across C.C is calculated using Eq. (7):

$$f = \frac{C_{p,g} \times (T_3 - 298) + C_{p,a} \times (298 - T_6)}{C_{p,g} \times (T_3 - 298) + H.V.} \tag{6}$$

$$\Delta P_{cc} = P_6 \times \frac{\Delta P_{cc}}{P_6} \tag{7}$$

d) Compressor Turbine (CT)

The temperature drop across the CT depends on turbine's efficiency (η_{ct}) and pressure ratio (r_{ct}) and is calculated using Eq. (8). The CT outlet temperature is calculated by Eq. (9) while the extracted work is calculated using Eq. (10):

$$\Delta T_{34} = T_3 \times \eta_{ct} \times \left(1 - \left(\frac{1}{r_{ct}} \right)^{\frac{k_g - 1}{k_g}} \right) \tag{8}$$

$$T_4 = T_3 * \left(1 - \Delta T_{34} / T_3 \right) \tag{9}$$

$$W_{ct} = W_c = m * C_{p,g} * \Delta T_{34} \tag{10}$$

e) Power Turbine (PT)

The temperature drop across the PT can be expressed by Eq. (11) while the turbine outlet temperature and the extracted work are calculated using Eq. (12) and Eq. (13), respectively.

$$\Delta T_{45} = T_4 \times \eta_{pt} \times \left(1 - \left(\frac{1}{r_{pt}} \right)^{\frac{k_g - 1}{k_g}} \right) \tag{11}$$

$$T_5 = T_4 \times \left(1 - \Delta T_{45} / T_4 \right) \tag{12}$$

$$W_{pt} = m \times C_{p,g} \times \Delta T_{45} \tag{13}$$

Matching GT Engine Components

The compressor and CT were matched based on three compatibility conditions: Work, rotational speed and mass flow rate. These conditions are expressed by Eq. (14), Eq. (15) and Eq. (16). The CT and PT are not mechanically connected, therefore only the mass flow compatibility condition given by Eq. (17) should be satisfied. The pressure ratios across each component, considering pressure losses across H. X and C.C, are related by Eq. (18). Equation (19) is used to calculate the power output of the GT engine:

$$\frac{\Delta T_{34}}{T_3} = \frac{\Delta T_{12}}{T_1} * \frac{T_1}{T_3} * \frac{C_{p,a}}{C_{p,g} * \eta_m} \tag{14}$$

$$\frac{N_c}{\sqrt{T_1}} = \frac{N_{ct}}{\sqrt{T_3}} \sqrt{\frac{T_3}{T_1}} \tag{15}$$

$$\frac{m\sqrt{T_3}}{P_3} = \frac{m\sqrt{T_1}}{P_1} * \frac{P_1}{P_2} * \sqrt{\frac{T_3}{T_1}} \tag{16}$$

$$\frac{m\sqrt{T_4}}{P_4} = \frac{m\sqrt{T_3}}{P_3} * \frac{P_3}{P_4} * \sqrt{\frac{T_4}{T_3}} \tag{17}$$

$$\frac{P_2}{P_1} = \frac{P_2}{P_6} * \frac{P_6}{P_3} * \frac{P_3}{P_4} * \frac{P_4}{P_5} * \frac{P_5}{P_7} \tag{18}$$

$$W_{gt} = W_{pt} = \dot{m} = C_{p,g} \times T_4 \times \mu_{pt} \times \left(1 - \left(\frac{1}{r_{pt}}\right)^{\frac{kg-1}{kg}}\right) \tag{19}$$

Figure 3 was produced using Eq. (19) to plot the change in GT engine power output as a function of the PT speed (N_{pt}) at different N_c values. The Specific Fuel Consumption (SFC) as well as the GT engine thermal efficiency ($\eta_{GT,th}$) are expressed by Eq. (20) and Eq. (21), respectively:

$$SFC = \frac{3600 \times f \times \dot{m}}{W_{net}} \tag{20}$$

$$\eta_{GT,th} = \frac{3600}{SFC \times H.V} \tag{21}$$

Matching the Centrifugal Pump and the Pipeline System

Matching the pump performance with the pipeline system requirements is presented in this subsection. Figure 4 shows two subsequent pressure-boosting stations (hypothetical) and illustrates the elevation difference between them, which is postulated by the nature of terrain characteristics.

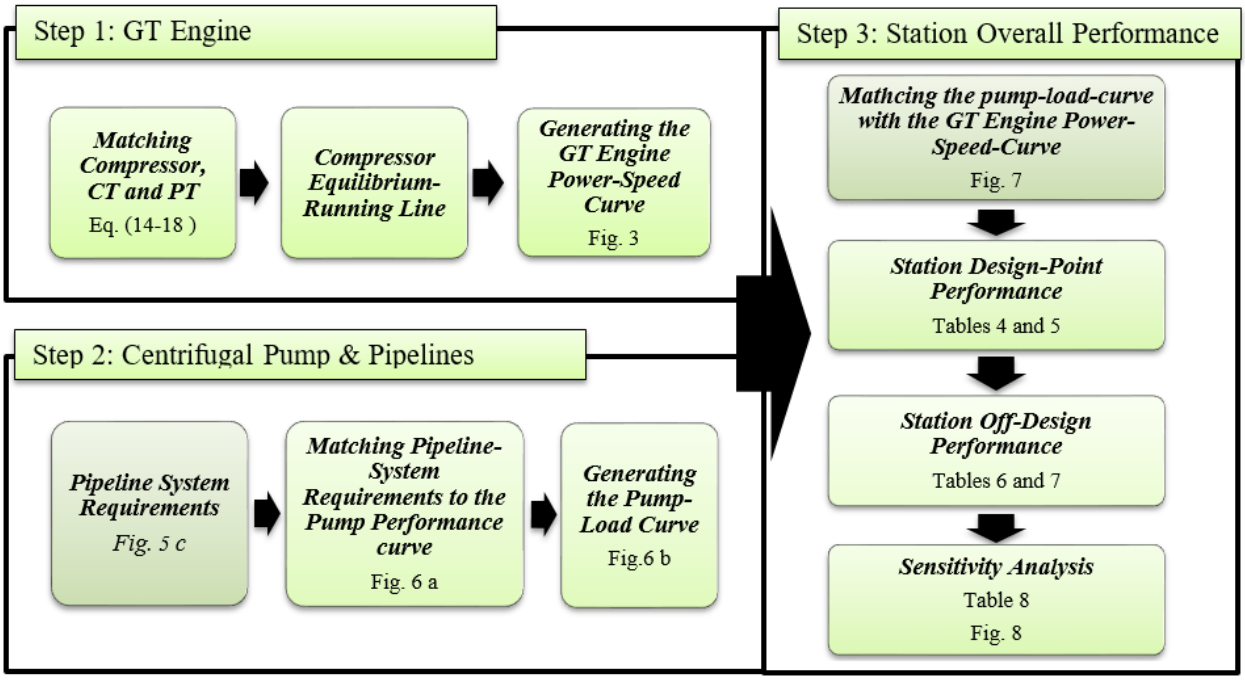

Fig. 2: Flowchart diagram summarizing the major steps of the modeling process

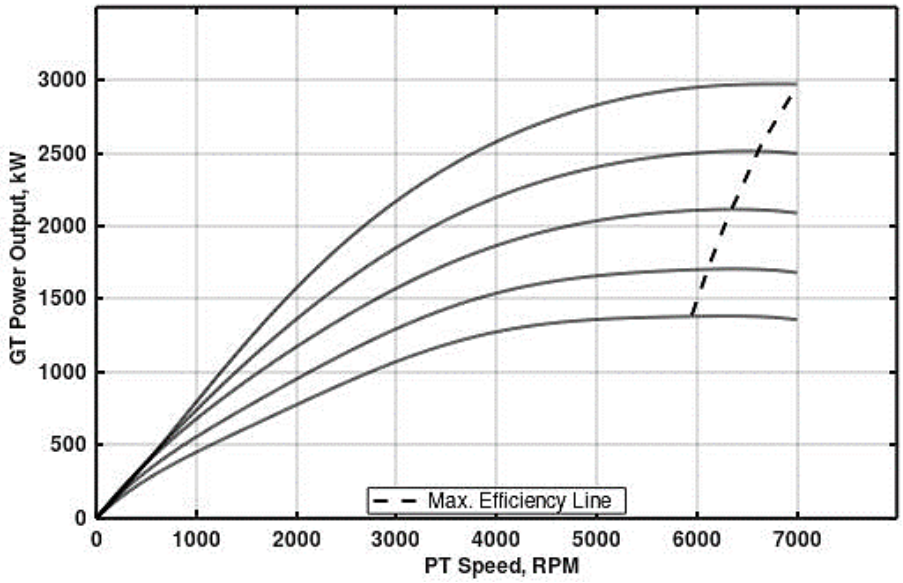

Fig. 3: GT engine power-speed curve at typical different Nc values.

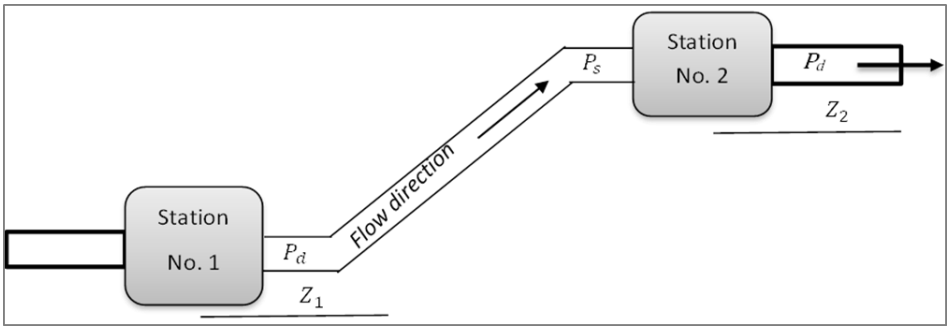

Fig. 4: Schematic diagram showing two hypothetical pressure-boosting stations on the same pipeline

The energy equation, Eq. (22), is applied between the discharge port of station 1 and the suction port of station 2 (Fox *et al*., 2012). When the liquid flows, the pressure drop (ΔP_i) is calculated using Eq. 23. The fluid velocity (V)is a function of the flow rate (Q) as described in Eq. (24). Equation (25) is used to generate the pipeline-system differential-head curve ($\Delta P/\gamma$), shown in Fig. 5:

$$\Delta P = \left(z_2 - z_1\right) \times \gamma + \Delta P_1 \tag{22}$$

$$\Delta P_1 = 0.0239 * \frac{\rho * \beta * L * V^2}{g * D} \quad where, V = \frac{4Q}{\pi D^2} \tag{23}$$

$$\Delta P_1 = 0.0239 * \frac{16}{\pi^2} * \frac{\rho * \beta * L * Q^2}{g * D^5} \tag{24}$$

$$\Delta P\gamma\left(z_2 - z_1\right) + 0.0239 * \frac{16}{\pi^2} * \frac{\rho * \beta * L * Q^2}{g * D^5} \tag{25}$$

The three-stage centrifugal pump provides the differential head ($\Delta P/\gamma$) required to compensate for the elevation head (Δz) and head loss ($\Delta Pi/\gamma$) along the length of the pipeline. The pressure rise (ΔP), pump output power and pump efficiency are expressed by Eq. (26, 27 and 28), respectively (Fox *et al*., 2012):

$$\Delta P = P_d - P_s \tag{26}$$

$$W_{p,out} = Q * \Delta P \tag{27}$$

$$\eta_p = W_{p,out} / W_{p,in} \tag{28}$$

The pipeline differential-head ($\Delta P/\gamma$) is matched with the pump-performance curve, as shown in Fig. 6a and the results of matching are used to generate the *pump-load curve* shown in Fig. 6b.

$$W_{p,in} = \Delta P \times Q \tag{29}$$

In a typical petroleum pipeline, the required pump discharge pressure is about 5900 KPa and the minimum suction pressure is about 500 KPa (Sawyer, 1976).

Matching the GT Power-Speed Curve with the Pump Load Curve

In this section, the *GT power-speed curve* (Fig. 3) and the *pump load curve* (Fig. 6b) are matched, and the result is shown in Fig. 7. The power input into the pump is related to the GT power output by Eq. (30), where (η_m) is the geartrain mechanical efficiency. The gearbox is chosen so that the design point on the pump-load curve is located on the GT engine maximum-efficiency-line. This condition is satisfied by applying Eq. (31), where R_{opt} is the optimum gearbox reduction ratio required to assure that the GT engine operates at maximum efficiency. Finally, the overall efficiency of the entire pressure-boosting plant (η_o) is expressed by Eq. (32):

$$W_{p,in} = W_{gt,out} \times \eta_m \tag{30}$$

$$R_{opt} = \frac{\left(\omega_{pt}\right)_{\max.efficiency}}{\left(\omega_p\right)_{dp}} \tag{31}$$

$$\eta_o = \eta_{gt} * \eta_m * \eta_p \tag{32}$$

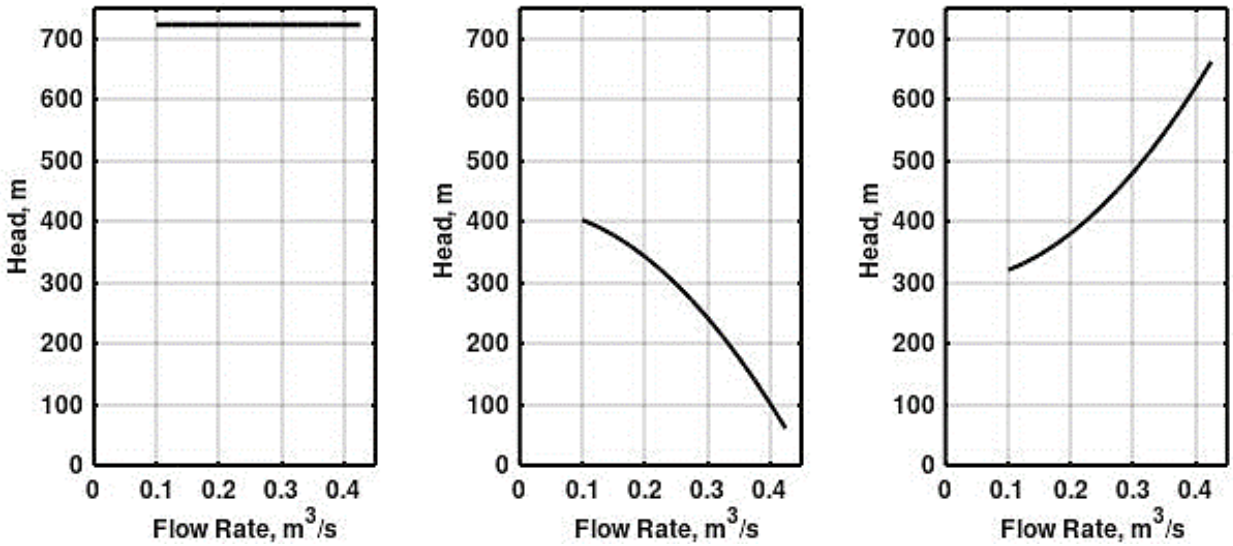

Fig. 5: Typical pipeline system head-flow curves: (a) discharge head, (b) suction head, (c) differential head

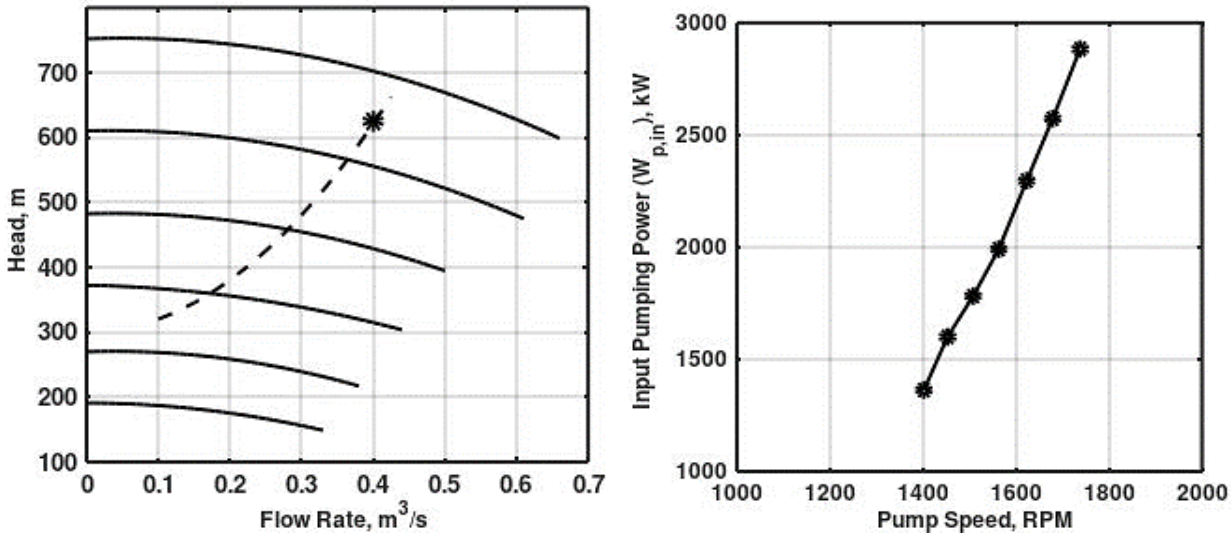

Fig. 6: (a) Pipeline-system differential-head curve matched to the pump-performance curve, (b) the pump load curve

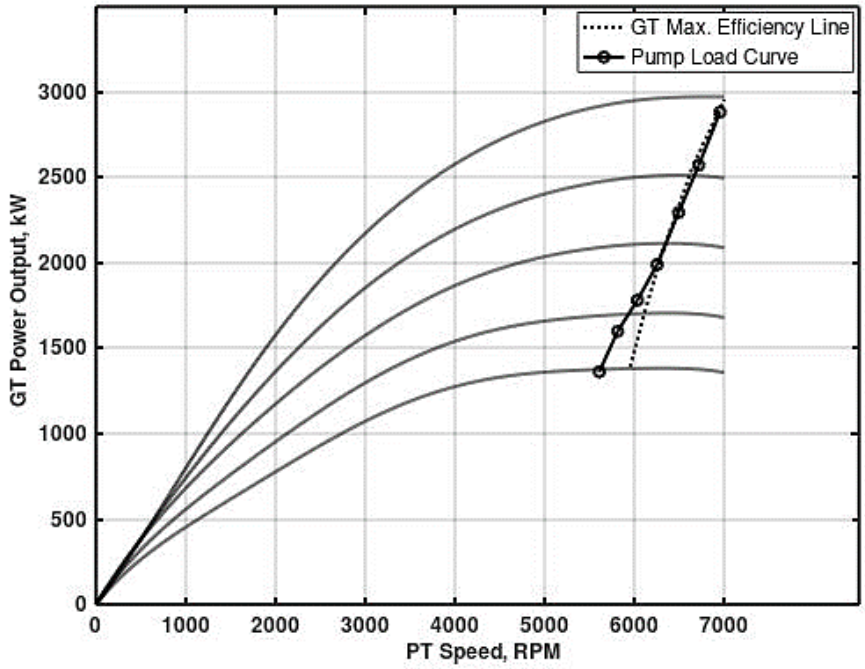

Fig. 7: Matching the pump load curve with the GT engine power-speed

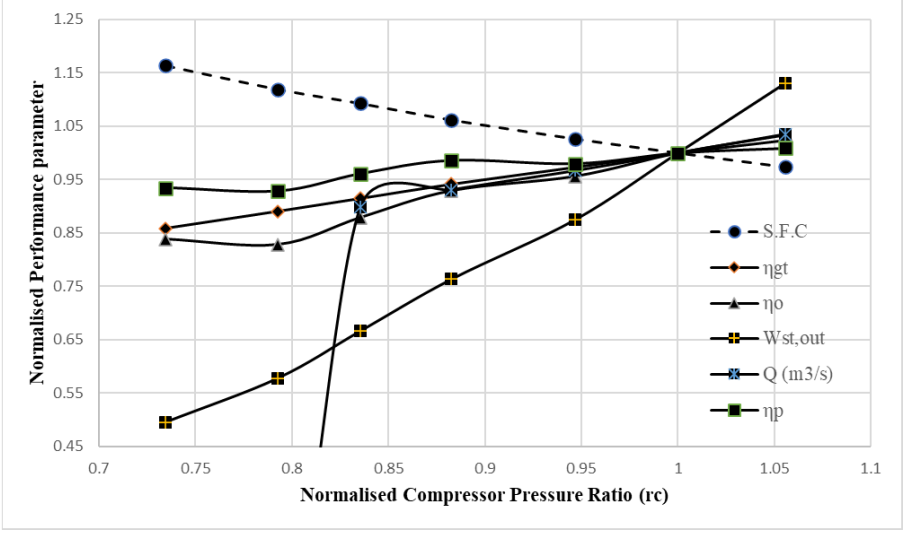

Fig. 8: The normalized effect of compressor pressure ratio (r_c) on the station performance parameters

Results and Discussion

Design Point Calculations

Table 2 shows the station performance parameters while Table 1 shows the properties, assumptions and operating conditions of the proposed pressure-boosting station at design point. It can be seen from Fig. 7 that the pump matches the GT engine near its *maximum-efficiency-line* over a wide loading range, which emphasizes the significance of employing the two-shaft GT design in variable speed applications. In fact, when the station runs near the GT *maximum-efficiency line*, the plant part-load efficiency is at its optimum value, thus the two-shaft GT engine is a very suitable prime mover for centrifugal pumps and compressors in many applications.

Off-Design Calculations

The station off-design behavior was investigated over the loading range specified along the pump load curve illustrated on Fig. 6b. It is clear from Fig. 7 that at higher

compressor pressure ratios (r_c), the pump-load-curve is perfectly matched with the GT engine maximum-efficiency-line. Table 3 shows the station off-design properties while Table 4 shows the station off-design performance parameters.

Non-dimensional analysis was carried out to study the effect of changing the compressor pressure ratio (r_c) on the plant performance parameters, mainly the GT engine efficiency (η_{gt}), the pump efficiency (η_p), the overall power output ($W_{st,ou}$) and the overall efficiency (η_{ov}). Figure 8 shows that as r_c increases, GT efficiency rises, and the station power output also increases at higher compression ratios. The station performance is enhanced at higher r_c values, since as the compression ration increases, the TIT increases. It is worth noting that references (Cohen *et al*., 1987; Najjar and Ismail, 1990) studied the effects of TIT and compression ratios (r_c) on the performance of a heat-exchange cycle, independently. They concluded that the efficiency increases with r_c and the power output increases significantly with TIT. Thus, increasing both r_c and TIT leads to higher GT engine efficiency and power output, as confirmed by the results indicated in Table 4 and Fig. 7. This result agrees with the conclusions in references (Cohen *et al*., 1987; Najjar and Ismail, 1990). Figure 8 also shows an increase in the pump efficiency with r_c, which is a logical result as the operation of the system moves from the low to the high efficiency region (points 1 to 7 on Fig. 6b) at higher loading conditions. This mainly relies on the nature of the pump performance-curve and pipeline differential-head-curve. Besides, the station overall efficiency (η_o) also increases with r_c since it is proportional to the efficiencies of both the pump (η_p) and the GT engine (η_{gt}) according to Eq. (25).

Sensitivity Analysis

To quantify the effect of varying the compressor pressure ratio (r_c) on the performance parameters of the pressure-boosting station, a sensitivity analysis was performed. Table 5 summarizes the change in each performance parameter for every 10% drop in r_c from its value at design-point.

Table 1: The properties and operating conditions of the oil-pipelines-pressure-boosting station, at design point

	Operating condition	Value
GT Engine Cohen *et al*. (1987)	Compressor Pressure Ratio, r_c	8.44
	Compressor Rotational Speed, N_c	97.95 %
	Compressor Isentropic. Efficiency, η_c	79 %
	Air Mass Flow Rate,	10.04 kg/s
	CT Pressure Ratio, r_{ct}	2.77
	CT Isentropic Efficiency, η_{ct}	85 %
	CT Inlet Temperature, T_3	1411 K
	PT Pressure Ratio, r_{pt}	3.06
	PT Rotational Speed, N_{pt}	6716 rpm
	PT Isentropic Efficiency, η_{pt}	0.850
	PT Inlet Temperature, T_4	K
	CT Inlet Temperature, T_3	1411 K
	Ambient Pressure, $p_a = p_1$	1 bar
	Ambient Temperature $T_a = T_1$	288 K
	Shaft Mechanical Efficiency, η_m	0.99
	Combustion Efficiency, η_b	0.99
	Pressure Drop across the Combustion Chamber, $\Delta p_{cc}/p_6$	0.03*P_d
	H.X Effectiveness, ϵ	0.85
	Pressure Drop across the H.X (air-side), $\Delta p_{ha}/p_2$	0.02*P_d
	Pressure Drop across the H.X (gas-side), Δp_{hg}	0.01 bar
Pump and Pipelines (Sawyer, 1976; Gilani *et al*., 2008)	Pump Head, H	625 m
	Pump Rotational Speed, N_p	1679 rpm
	Volume Flow Rate, Q_d	0.400 m^3/s
	Suction Pressure, P_s	800 kPa
	Minimum Suction Pressure, $p_{s,min}$	*500 kPa*
	Delivery (Discharge) Pressure, p_d	*5900 kPa*
	Pipeline Length, L	*1000 km*
	Pipeline Diameter, D	*0.381 m*
	Pipe Friction Factor, β	*0.04*
	Elevation Difference, z_2-z_1	*300 m*
Oil Liquid Properties (Diesel) Liquids - Kinematic Viscosities (2018)	Avg. Specific Weight, γ	*8162 N/m^3*
	Avg. Density, ρ	*832 kg/m^3*
	Avg. Dynamic Viscosity, μ	*0.0248 Pa.s*
	Heating Value, H.V	*42517 kJ/kg*

Table 2: The performance parameters of the oil-pipelines-pressure-boosting station, at design point

GT Engine	GT Power Output, $W_{gt,out}$	2599 kW
	GT Efficiency, η_{gt}	37.5%
		0.217 *kg/kWh*
Pump	Specific Fuel Consumption, SFC	2573 kW
	Pump power input, W_p	79.3%
Overall Station	Station power output, W_{ov}	2040 kW
	Station efficiency, η_{ov}	29.7%

Table 3: The station off-design properties at different r_c values corresponding to the points along the pump-load-curve shown in Fig. 6b

	GT Engine											
	Compressor				CT		PT			Pump		
	#	r_c	N_c(%)	$\dot{m}_{air}\,(kg/s)$	r_{ct}	TIT (K)	N_{pt} (rpm)	r_{pt}	ηpt (%)	N_p (rpm)	H (m)	Q (m^3/s)
Part Load	1	6.20	90.05	8.12	2.63	1190	5608	2.22	84.7	1402	450	0.275
	2	6.69	91.78	8.54	2.67	1238	5812	2.35	84.7	1453	481	0.300
	3	7.05	93.05	8.85	2.70	1274	6032	2.46	84.9	0.325	512	1508
	4	7.45	94.44	9.18	2.72	1313	6252	2.57	85.0	0.350	545	1563
	5	7.99	96.35	9.65	2.75	1367	6492	2.74	85.0	0.375	583	1623
Design Point	6	8.44	97.95	10.04	2.76	1411	6716	2.88	85.0	0.400	625	1679
Overload	7	8.91	99.61	10.44	2.78	1458	6952	3.03	85.0	0.425	665	1738

Table 4: The station off-design performance at different r_c values corresponding to the points along the pump-load-curve shown in Fig. 6b

			GT Engine		*Pump*		*Overall Performance*		
	#	r_c	$W_{gt,out}$ *(kW)*	*SFC (kg/kWh)*	*(%)*	*(kW)*	*(%)*	*(kW)*	*(%)*
Part Load	1	6.20	1377	0.263	32.2	1363	74.1	1010	24.9
	2	6.69	1616	0.253	33.4	1600	73.6	1178	24.6
	3	7.05	1800	0.247	34.3	1782	76.2	1358	26.1
	4	7.45	2011	0.240	35.3	1991	78.2	1557	27.6
	5	7.99	2320	0.232	36.5	2296	77.7	1784	28.4
Design Point	6	8.44	2600	0.226	37.5	2573	79.3	2040	29.7
Overload	7	8.91	2913	0.220	38.4	2883	80.0	2307	30.7

Table 5: The amount of change in performance parameters for every 10% drop in compressor pressure ratio (r_c)

(r_c)	Q	W_{st}	η_{gt}	η_p	η_o
-10%	- 11%	- 21%	- 5%	- 1.5%	- 6.5%

Conclusion

- The GT engine components were optimally matched to generate the GT engine maximum-efficiency-line
- The pump performance was matched with the pipeline-system requirements to generate the pump load-curve
- The pump load-curve was matched to the GT engine power-speed-curve along its maximum-efficiency-line
- The station net power output and specific fuel consumption were 2 MW and 0.217 kg/kWh, respectively
- Efficiencies of the GT engine, pump and the entire station at D.P were 37.5, 79.3 and 29.7%, respectively
- At 50% power-output loading from D.P, the GT engine part-load efficiency was 32.2% (Table 4)
- At 50% power-output loading from D.P, the pressure ratios of the compressor, CT and PT were reduced by 27, 4.7 and 26.7%, respectively. Hence, the CT operating range is the most limited (Table 3)
- For a 10% drop in r_c from D.P, the station overall efficiency drops by only 6.5% (Table 5)

Acknowledgement

This paper is devoted to the memory of Professor Yousef Najjar who passed away on the 7th of March 2021.The authors would also like to thank the DAAD association for supporting and funding the study of the third author.

Author's Contributions

Yousef S. H. Najjar: Developed the concept and the research idea.

Mohammad Z. M. Yousef: Performed the modelling, simulation, obtained the results and wrote the initial draft.

Aad M. A. Al-Mahgari: Wrote the final manuscript, revised and prepared it for publication.

Ethics

This research does not contain any studies involving human or animal participants performed by any of the authors.

This research paper is original and all authors have read and approved it and there are no ethical issues related.

References

Aklilu, B. T., & Gilani, S. I. (2010). Mathematical modeling and simulation of a cogeneration plant. Applied Thermal Engineering, 30(16), 2545-2554. doi.org/10.1016/j.applthermaleng.2010.07.005

Akyurt, M., Lamfon, N. J., Najjar, Y. S. H., Habeebullah, M. H., & Alp, T. Y. (1995). Modeling of waste heat recovery by looped water-in-steel heat pipes. International journal of heat and fluid flow, 16(4), 263-271. doi.org/10.1016/0142-727X(94)00023-6

Al-Hamdan, Q. Z., & Ebaid, M. S. (2006). Modeling and simulation of a gas turbine engine for power generation. doi.org/10.1115/1.2061287

Barigozzi, G., Perdichizzi, A., Gritti, C., & Guaiatelli, I. (2015). Techno-economic analysis of gas turbine inlet air cooling for combined cycle power plant for different climatic conditions. Applied Thermal Engineering, 82, 57-67. doi.org/10.1016/j.applthermaleng.2015.02.049

Bensakhria, A., Peysson, Y., & Antonini, G. (2004). Experimental study of the pipeline lubrication for heavy oil transport. Oil & gas science and technology, 59(5), 523-533. doi.org/10.2516/ogst:2004037.

Chapman, J. W., Lavelle, T. M., & Litt, J. S. (2016). Practical techniques for modeling gas turbine engine performance. In 52nd AIAA/SAE/ASEE joint propulsion conference (p. 4527). doi.org/10.2514/6.2016-4527.

Cohen, H., Rogers, G. F. C., & Saravanamutto, H. I. H. (1987). Gas Turbine Theory, Longman Scientific & Technical.

Fox, R. W., McDonald, A. T., Pritchard, P. J. (2012). Fluid Mechanics. 8th ed. John Wiley & Sons Inc.; 2012.

Gilani, S. I. U. H., Baheta, A. T., Majid, A., & Amin, M. (2008). Thermodynamics approach to determine a gas turbine components design data and scaling method for performance map generation.

Gudala, M., Banerjee, S., Naiya, T. K., Mandal, A., Subbaiah, T., & Rao, T. R. M. (2019). Hydrodynamics and energy analysis of heavy crude oil transportation through horizontal pipelines using novel surfactant. Journal of Petroleum Science and Engineering, 178, 140-151. doi.org/10.1016/j.petrol.2019.03.027.

Guo, Y., Meng, X., Wang, D., Meng, T., Liu, S., & He, R. (2016). Comprehensive risk evaluation of long-distance oil and gas transportation pipelines using a fuzzy Petri net model. Journal of Natural Gas Science and Engineering, 33, 18-29. doi.org/10.1016/j.jngse.2016.04.052.

Hart, A. (2014). A review of technologies for transporting heavy crude oil and bitumen via pipelines. Journal of Petroleum Exploration and Production Technology, 4(3), 327-336. doi.org/10.1007/s13202-013-0086-6.

Bălănescu, D. T., & Homutescu, V. M. (2019). Performance analysis of a gas turbine combined cycle power plant with waste heat recovery in Organic Rankine Cycle. Procedia Manufacturing, 32, 520-528. doi.org/10.1016/j.promfg.2019.02.248

Koch, G., Ayello, F., Khare, V., Sridhar, N., & Moosavi, A. (2015). Corrosion threat assessment of crude oil flow lines using Bayesian network model. Corrosion Engineering, Science and Technology, 50(3), 236-247. doi.org/10.1179/1743278215Y.0000000005.

Liquids - Kinematic Viscosities. (2018). Engineering Toolbox [was available on. http://www.engineeringtoolbox.com

Mallinson, D. H., & Lewis, W. G. E. (1948). The part-load performance of various gas-turbine engine schemes. Proceedings of the Institution of Mechanical Engineers, 159(1), 198-219. doi.org/10.1243/PIME_PROC_1948_159_019_02

Martínez-Palou, R., de Lourdes Mosqueira, M., Zapata-Rendón, B., Mar-Juárez, E., Bernal-Huicochea, C., de la Cruz Clavel-López, J., & Aburto, J. (2011). Transportation of heavy and extra-heavy crude oil by pipeline: A review. Journal of petroleum science and engineering, 75(3-4), 274-282. doi.org/10.1016/j.petrol.2010.11.020

Najjar, Y. S. H., & Ismail, M. S. (1990). Optimum pressure ratios for different gas turbine cycles. High Temperature Technology, 8(4), 283-289. doi.org/10.1080/02619180.1990.11753494.

Najjar, Y. S. H., Akyurt, M., Al-Rabghi, O. M., & Alp, T. (1993). Cogeneration with gas turbine engines. Heat Recovery Systems and CHP, 13(5), 471-480. doi.org/10.1016/0890-4332(93)90048-Z.

Najjar, Y. S., & Abubaker, A. M. (2015). Indirect evaporative combined inlet air cooling with gas turbines for green power technology. International journal of refrigeration, 59, 235-250. doi.org/10.1016/j.ijrefrig.2015.07.001.

Poullikkas, A. (2005). An overview of current and future sustainable gas turbine technologies. Renewable and Sustainable Energy Reviews, 9(5), 409-443. doi.org/10.1016/j.rser.2004.05.009.

Sawyer, J. W. (1976). Gas Turbine Engineering Handbook. Gas Turbine Publications; 1976.

Smooth Turbine Maps. (2018). [computer software] [available on www.gasturb.de/software]

Turbocompressor. (2016). Louisiana Chemical Equipment Company. http://www.lcec.com/

Wang, B., Zhang, H., Yuan, M., Wang, Y., Menezes, B. C., Li, Z., & Liang, Y. (2019). Sustainable crude oil transportation: Design optimization for pipelines considering thermal and hydraulic energy consumption. Chemical Engineering Research and Design, 151, 23-39. doi.org/10.1016/j.cherd.2019.07.034

Nomenclature:

Symbols:	**Subscripts:**		
C	Compressor	a	Ambient
C.C	Combustion Chamber	c	Compressor
Con	Condenser	cc	Combustion Chamber
CT	Compressor Turbine	ct	Compressor Turbine
D	Pipeline Diameter (m)	d	Discharge Port
D.P	Design point	dp	Design Point
F	Fuel-to-Air Ratio	g	Gas
GB	Gearbox	gb	Gear Box
GT	Gas Turbine	gt	Gas Turbine
H	Pump Head (m)	l	Losses
HV	Fuel Heating Value (kJ/kg)	m	Mechanical
HRSG	Heat Recovery Steam Generator	o	Overall
L	Pipeline Length (km)	p	Pump
$\dot{m}$	Mass Flow Rate (kg/s)	pt	Power Turbine
N	Rotational Speed (rpm)	s	Suction Port
p	Pressure (bar)	th	Thermal
PT	Power Turbine	Greek Letters:	
Q	Pump volume Flow Rate (m^3/s)	β	Pipeline friction factor
R	Gear Ratio	γ	Specific gravity (N/m^3)
r	Pressure Ratio	ε	Effectiveness
SFC	Specific Fuel Consumption (kg/kWh)	η	Efficiency
ST	Steam Turbine	μ	Dynamic Viscosity (Pa.s)
T	Temperature (K)	ρ	Density (kg/m^3)
V	Velocity (m/s)	ω	Rotational Speed (rpm)
W	Work (kW)	Δ	Change
z	Elevation (m)		